PNAS RESEARCH ARTICLE | NEUROSCIENCE OPEN ACCESS

Fear circuit–based neurobehavioral signatures mirror resilience to chronic social stress in mouse

Sarah Ayash[a,b], Thomas Lingner[c], Anna Ramisch[d], Soojin Ryu[e,f], Raffael Kalisch[a,g], Ulrich Schmitt[a,b,1], and Marianne B. Müller[a,b,1,2]

Edited by Huda Akil, University of Michigan-Ann Arbor, Ann Arbor, MI; received March 31, 2022; accepted March 9, 2023

Consistent evidence from human data points to successful threat–safety discrimination and responsiveness to extinction of fear memories as key characteristics of resilient individuals. To promote valid cross-species approaches for the identification of resilience mechanisms, we establish a translationally informed mouse model enabling the stratification of mice into three phenotypic subgroups following chronic social defeat stress, based on their individual ability for threat–safety discrimination and conditioned learning: the *Discriminating-avoiders*, characterized by successful social threat–safety discrimination and extinction of social aversive memories; the *Indiscriminate-avoiders*, showing aversive response generalization and resistance to extinction, in line with findings on susceptible individuals; and the *Non-avoiders* displaying impaired aversive conditioned learning. To explore the neurobiological mechanisms underlying the stratification, we perform transcriptome analysis within three key target regions of the fear circuitry. We identify subgroup-specific differentially expressed genes and gene networks underlying the behavioral phenotypes, i.e., the individual ability to show threat–safety discrimination and respond to extinction training. Our approach provides a translationally informed template with which to characterize the behavioral, molecular, and circuit bases of resilience in mice.

mouse model | threat–safety discrimination | extinction | fear circuit | transcriptional signatures

Significance

Mice evaluate interaction with conspecifics by their potential for harm or benefit. Similarly, the ability to discriminate social stimuli is of fundamental importance in humans: A delicate balance between fear response generalization and discrimination can promote resilience in an ever-changing world. Here, we establish a translationally informed approach to detect resilience versus susceptibility to social defeat stress. We capitalize on the individual ability of mice to discriminate between threat and safe stimuli under stressful conditions, and their response to extinction. We identify a behavioral phenotype of resilience supported by unique transcriptional signatures in specific nuclei of the fear circuitry. Our approach might serve as a blueprint for advancing the development of prevention strategies against stress-related mental disorders.

Despite decades of research on stress-related mental disorders, their prevalence remains high (1). This has inspired an approach that is complementary to disease-oriented research and has resilience at its core (2–4). Stress resilience is defined as the maintenance or quick recovery of mental health during and after adversity (3). Recent global challenges such as the coronavirus disease-2019 (COVID-19) pandemic (5), war, and displacement of nations are threatening the mental health of millions. During recent years, considerable efforts have been undertaken to define valid phenotypes and outcomes of resilience in human research (6). Of importance, human research points to a specific role of successful threat–safety discrimination and responsiveness to extinction of fear memories in resilience (7). Healthy subjects have been found to express fear in response to a threat-associated cue but do not respond or respond less to a safety cue (8–13). In contrast, anxiety disorders, e.g., posttraumatic stress disorder, are characterized by generalized fear that is associated with a negative impact on mental health (12, 14–17). Meanwhile, research on extinction suggests that anxiety patients show delayed and reduced fear extinction compared to healthy subjects (7). The neurocircuitry of fear conditioning and extinction shows a high degree of evolutionary conservation across many species. We propose that a mouse model that assesses the individual ability for threat–safety discrimination and responsiveness to extinction following stress would be best suited to investigate translationally relevant resilience mechanisms.

Previously, we have identified the crucial involvement of conditioned learning in the *Chronic Social Defeat* (CSD) mouse model (18). We showed that on a group level, CSD-induced social avoidance (a widely used outcome measure) i) is specific toward the phenotypic characteristics of the aggressors' strain (attacking strain during CSD days) and does not generalize to different mouse strains and ii) can be reversed following extinction training involving repeated but safe (without physical attacks) exposure to individual mice from the aggressors' strain. This aspect of avoidance specificity toward the aggressor strain was recently followed up and confirmed in an independent study (19).

While group-level analysis indicated intact threat–safety discrimination and responsiveness to extinction, we also observed substantial variability (18). To precisely assess an individual animal's ability for threat–safety discrimination, we designed the *Social Threat-Safety Test* (STST; previously referred to as the *Modified Social Interaction Test;* ref. 18) where the experimental mouse is offered the choice to freely interact with the threat-associated cue (aggressors' strain) and a safe cue (novel strain) following CSD (18). Moreover, to confirm that social avoidance in the STST is an aversive conditioned

Competing interest statement: The authors have organizational affiliations to disclose, Raffael Kalisch received advisory honoraria from JoyVentures.

This article is a PNAS Direct Submission.

[1]U.S. and M.B.M. contributed equally to this work.

[2]To whom correspondence may be addressed. Email: marianne.mueller@lir-mainz.de.

This article contains supporting information online at https://www.pnas.org/lookup/suppl/doi:10.1073/pnas.2205576120/-/DCSupplemental.

Published April 17, 2023.

response, we expand here our analyses with an additional operant conditioning experiment in mice first subjected to CSD and STST. We hypothesize that the interindividual differences in the STST will be mirrored by interindividual differences in the unrelated operant conditioning experiment. In a separate cohort of mice, we test whether interindividual differences in the STST will correspond to interindividual differences in responsiveness to a subsequent extinction training. To explore the neurobiological mechanisms underlying the behavioral signatures observed in the STST, we further investigate whether the identified subgroups are characterized by unique differentially expressed genes (DEGs) and gene networks in classical fear conditioning- and anxiety-related brain regions, namely basolateral amygdala (blA), ventral hippocampus (vHC), and medial prefrontal cortex (mPFC).

Results

The STST Identifies Three Distinct Phenotypes within a Single Defeated Group. Based on the calculation of two social interaction indices in the STST (Fig. 1 *A* and *B*), one for each cue (strain), we identified three distinct phenotypic subgroups within the single *Defeated* group: Mice with a social interaction index ≥1 with the threat-associated cue (aggressors' strain) were labeled *Non-avoiders*, mice with a social interaction index <1 with both cues were labeled *Indiscriminate-avoiders,* and mice with a social interaction index ≥1 exclusively with the safe cue (novel strain) were labeled *Discriminating-avoiders* (Fig. 1 *C* and *D*). Nondefeated *Control* mice had similar indices with both strains. For additional analyses, see *SI Appendix*, Fig. S1 *A* and *B*.

Based on the importance of threat–safety discrimination for resilience in humans, which correlates with responsiveness to extinction, we hypothesize the following: 1) The *Non-avoiders*' social interaction with the aggressors' strain reflects an inappropriate aversive conditioned response toward the threat-associated cue, and thus impaired aversive conditioned learning relative to the other two subgroups. 2) The *Indiscriminate-avoiders*' social avoidance toward the aggressors' strain reflects intact aversive conditioned learning; however, social avoidance of the novel strain reflects a generalized aversive conditioned response toward a safe cue, i.e., failed threat–safety discrimination, rendering this subgroup susceptible to stress-related dysfunctions; 3) The *Discriminating-avoiders'* social avoidance exclusively toward the aggressors' strain reflects intact aversive conditioned learning, whereas social interaction with the novel strain reflects successful threat–safety discrimination. This subgroup may mimic resilience

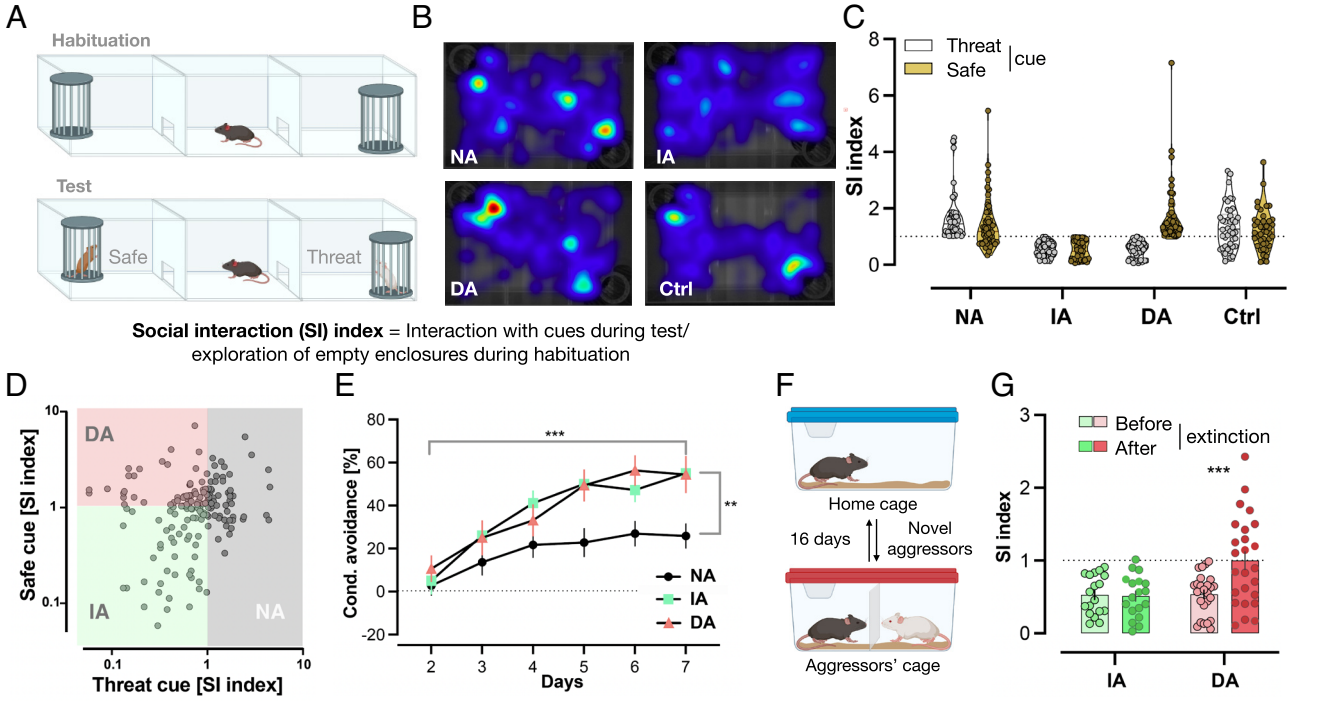

Fig. 1. The STST identifies three distinct phenotypes within a defeated group. (*A*) STST: Following the habituation phase, the testing phase took place where two novel cues were presented with one belonging to the same strain that defeated the mice during CSD days (threat), while the other belonging to a novel strain (safe). (*B*) Differing occupancy of areas within the arena between the different subgroups: Representative heatmaps of each subgroup during the testing phase of STST. Darker colors indicate more time spent in the area. (*C*) STST identifies three phenotypic subgroups within a single defeated group: Mice with a social interaction index ≥1 with the threat-associated cue were termed *Non-avoiders* (NA; n = 55), mice with a social interaction index <1 with both strains were termed *Indiscriminate-avoiders* (IA; n = 54), and mice with a social interaction index ≥1 *only* with the safe cue were termed *Discriminating-avoiders* (DA; n = 56). Nondefeated *Control* (Ctrl; n = 42) had similar indices with both strains. Results are presented as truncated violin plots. Each animal is represented by two data points, one with each cue. (*D*) Scatter plot of the same data from *C*. (*E*) *Non-avoiders* show impairment in conditioned learning of aversive cues: All *Defeated* subgroups had a significant increase in conditioned avoidance response% throughout the training days; however, the *Non-avoiders* did so to a lesser extent with a significantly lower value on the seventh (last) day compared to the other two subgroups. Results are presented as mean ± SEM, two-way ANOVA, days: F (5, 160) = 46.27, $P < 0.0001$***, subgroups: F(2, 32) = 4.359, $P = 0.0212$*, interaction: F(10, 160) = 3.042, $P = 0.0015$**. Bonferroni's multiple comparisons test on last day: DA (n = 8) vs. IA (n = 9), P = ns, DA or IA vs. DA (n = 18), $P < 0.01$**. (*F*) *Social Avoidance Extinction Training:* Mice were placed for 15 min in the same cages of the same aggressors from CSD days with a mesh wall in-between before being returned to their home cages. The training took place for 16 d; every day, a new aggressor was encountered. (*G*) *Indiscriminate-avoiders* display resistance to extinction of averse memories: The DA (n = 25) had a significantly greater social interaction (SI) index with the aggressors' strain in the STST following extinction training compared to their index in the test before the training (following CSD), whereas the IA (n = 18) maintained similar indices between both time points. Results are presented as mean ± SEM, two-way ANOVA, extinction training: F (1, 41) = 7.092, $P = 0.0110$**, subgroups: F(1, 41) = 7.061, $P = 0.0112$**, interaction: F(1, 41) = 8.293, $P = 0.0063$**, and Bonferroni's multiple comparisons test within each subgroup: before vs. after extinction, $P = 0.0002$***.

in humans, i.e., individuals that remain functional after stress exposure. *SI Appendix*, Fig. S2 represents a schematic timeline.

Non-Avoiders Show Impairment in Conditioned Learning of Aversive Cues. According to our hypotheses (1–3), if the STST reflects true ability, or lack thereof, to learn an aversive cue, then these individual behavioral differences should extend to aversive nonsocial cues. Accordingly, a cohort of mice from each of the three *Defeated* subgroups following CSD and STST underwent the *Active Avoidance Task*.

The conditioned avoidance increased in all subgroups throughout the training days (Fig. 1*E*). However, the *Non-avoiders* subgroup did so to a lesser extent. At day seven (last day), this subgroup's avoidance was significantly lower compared to that of the other two subgroups. Similar results were found for avoidance/escape ratio (*SI Appendix*, Fig. S3*A*). Importantly, the only subgroup not to reach a conditioned avoidance response above chance level (50%) on the last day was the *Non-avoiders* (*SI Appendix*, Table S1), suggesting that this is the only subgroup that failed to learn the task. Furthermore, conditioned avoidance response on the last day of the *Active Avoidance Task* and social interaction indices with the aggressors' strain in the STST showed a significant negative correlation (Pearson's correlation, r = –0.3872, $P = 0.0237$*, n = 34). Finally, we ruled out potential differences in pain threshold between the three *Defeated* subgroups that could influence the results (*SI Appendix*, Fig. S3B and *SI Text*). Together, these results suggest that social avoidance of the aggressors' strain reflects intact learning of threat-associated cues. In contrast, maintaining normal levels of interaction with the aggressors' strain, as seen in the *Non-avoiders* subgroup, is a reflection of impaired aversive conditioned learning, supporting our hypotheses (1–3).

Indiscriminate-Avoiders Display Resistance to Extinction. Intact threat–safety discrimination ability and responsiveness to extinction in resilient individuals (7) suggest that these behavioral phenotypes maybe coupled. We, therefore, conducted a recently introduced *Social Avoidance Extinction Training* (Fig. 1F and ref. 18). We hypothesized that among the two *Defeated* subgroups that acquire social avoidance behavior during CSD (*Indiscriminate-* and *Discriminating-avoiders*), only the subgroup with successful threat–safety discrimination (*Discriminating-avoiders*) would respond to extinction (hypotheses 2–3).

Indiscriminate- and *Discriminating-avoiders* both avoided the aggressors' strain in the first STST following CSD (Fig. 1*G*). Notably, the STST following the extinction training revealed that *only* the *Discriminating-avoiders* successfully extinguished their social avoidance toward the threat-associated cue, whereas the *Indiscriminate-avoiders* were resistant to extinction, supporting hypotheses 2–3 (Fig. 1*G*). Fig. 2 represents a conceptual graphical overview.

To explore the molecular mechanisms underlying the behavioral signatures observed in the STST, we performed transcriptome analysis in the blA, vHC, and mPFC.

Subgroup- and Brain Region-Specific DEGs. We tracked subgroup-specific DEGs relative to the nondefeated *Control* group and to the other *Defeated* subgroups (*SI Appendix*, Fig. S4; for a complete overview of the results, see Dataset S1). In the blA, we identified four genes specific to the *Indiscriminate-avoiders* subgroup (Fig. 3). In the mPFC, 14 genes were specific to the *Indiscriminate-avoiders* subgroup and 12 genes for the *Non-avoiders* subgroup (Fig. 3). DEGs specific for the *Indiscriminate-avoiders* subgroup include, among others, several hemoglobin-related genes and genes involved in vascular function. In the vHC, one gene was specific to the *Indiscriminate-avoiders* subgroup and a group of five DEGs was specific to the *Discriminating-avoiders* subgroup (Fig. 3). To investigate which subgroups are more similar to each other, we performed Spearman's correlation analysis where we directly compared the effect sizes (log2fold changes) for the different subgroups using the 1,000 most variable genes across all subgroups (*SI Appendix*, Fig. S5).

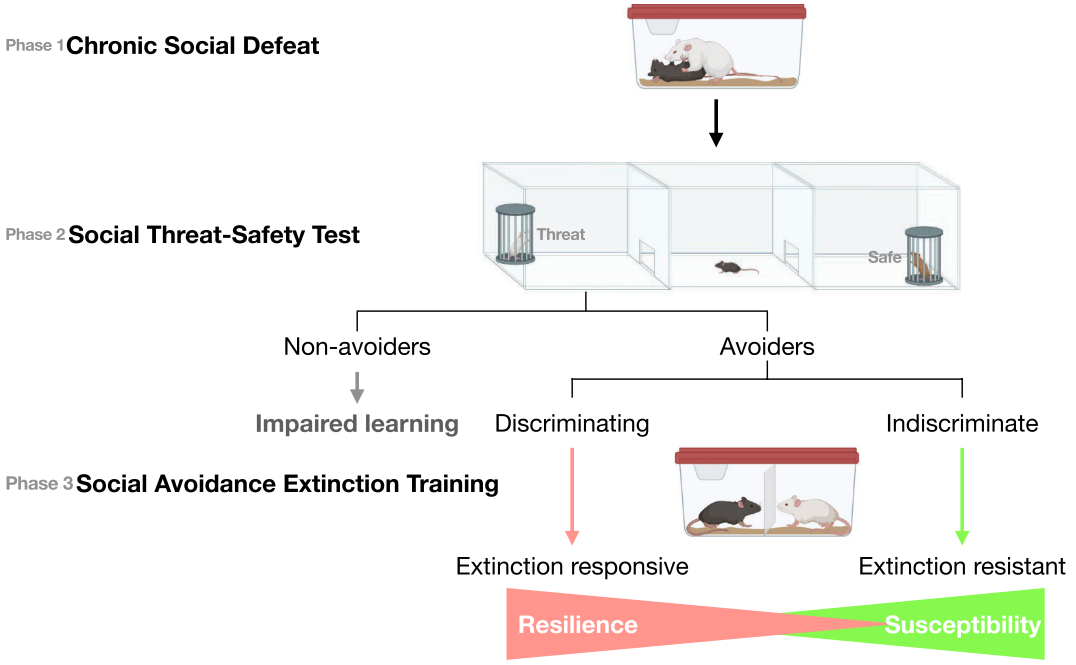

Fig. 2. Conceptual graphical overview. Following CSD and employing the STST, the single *Defeated* group is stratified based on social avoidance development toward the threat-associated cue (conditioned learning of aversive cues). The single subgroup of avoiders is further stratified based on social avoidance development toward the safe cue (threat–safety discrimination). The *Discriminating-avoiders* do not display social avoidance toward the safe cue and thus are characterized by successful threat–safety discrimination as well as responsiveness to *Social Avoidance Extinction Training* (extinction of aversive memories). In line with research in humans, they express resilience after adversity. In contrast, the *Indiscriminate-avoiders* display social avoidance toward the safe cue and thus are characterized by aversive response generalization to safe stimuli as well as resistance to extinction, reflecting stress susceptibility. Finally, the *Non-avoiders* are characterized by an impaired ability to conditionally learn aversive cues, thus are out of the "resilience susceptibility" spectrum.

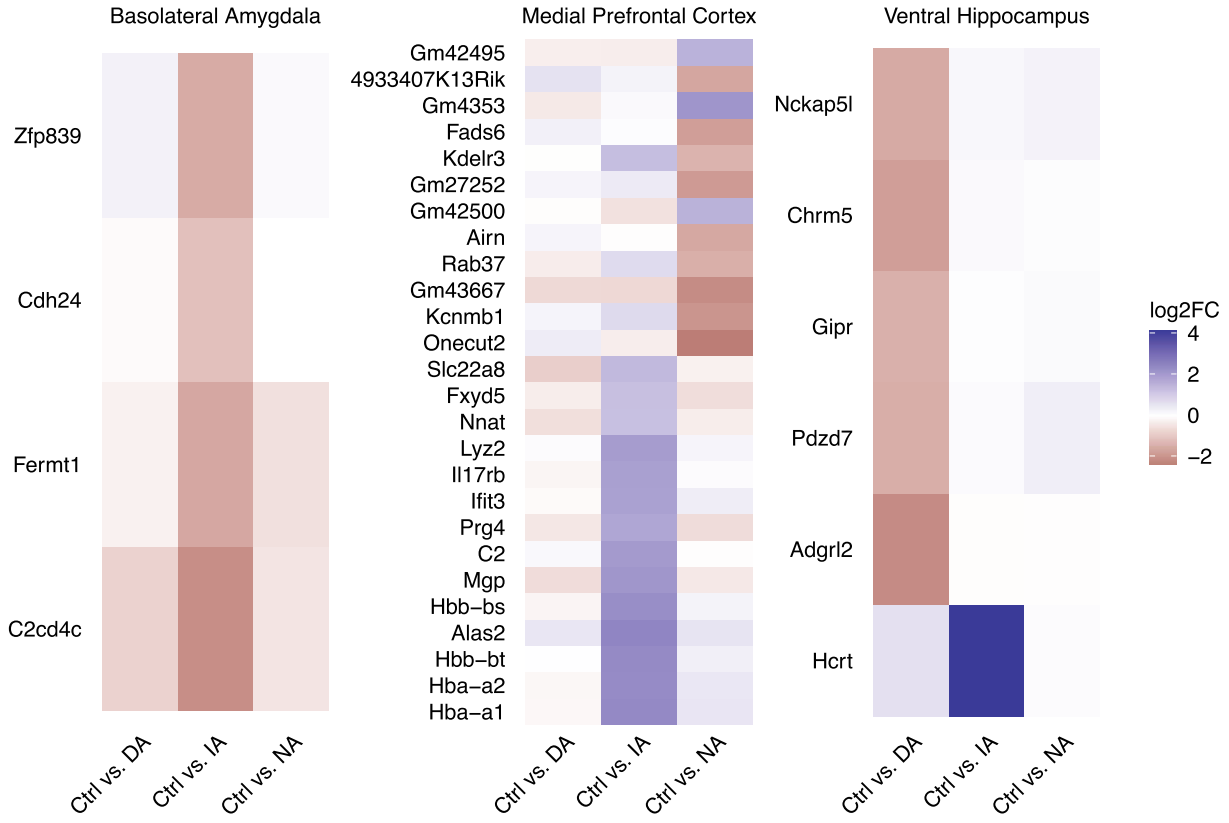

Fig. 3. Subgroup- and brain region-specific DEGs. Heatmaps of identified subgroup-specific DEGs in blA, mPFC, and vHC: For each region, change of gene expression between the nondefeated *Control* group (Ctrl) and each of the three *Defeated* subgroups is shown. The color code represents the log2 fold change of the average normalized gene expression where blue values indicate greater expression in the respective *Defeated* subgroup compared to the *Control* group. *Discriminating-avoiders* (DA), *Indiscriminate-avoiders* (IA), and *Non-avoiders* (NA), n = 4 to 7 per subgroup.

In the blA, there was a high correlation between *Discriminating-avoiders* and *Non-avoiders* subgroups (*SI Appendix*, Fig. S5*A*). In contrast, there was a low correlation between *Indiscriminate-avoiders* subgroup and the two other subgroups (*SI Appendix*, Fig. S5*A*). In the mPFC, there was a moderate correlation between all subgroup comparisons (*SI Appendix*, Fig. S5*B*). In the vHC, correlation between *Discriminating-avoiders* and *Non-avoiders* subgroups was low, while between *Indiscriminate-avoiders* subgroup and the other two subgroups, it was moderate (*SI Appendix*, Fig. S5*C*).

Subgroup-Specific Gene Coexpression Networks. We employed weighted gene coexpression network analysis (WGCNA) to identify specific modules of genes that correlate across brain regions and could be critical in determining the subgroups (Fig. 4). In this analysis, genes that show a similar expression pattern across all the three brain regions within each of the three *Defeated* subgroups and the *Control* group are clustered into modules. The *Non-avoiders* network consisted of 94 modules, the *Indiscriminate-avoiders* network consisted of 140 modules, the *Discriminating-avoiders* network consisted of 118 modules, and the *Control* network consisted of 87 modules (note the networks are independent and the module names, though reused, do not imply similarity of gene members; Fig. 4*A*). Enrichment analysis of the identified coexpression modules was performed to probe the biological relevance of the modules and identify significant subgroup-specific (exclusive) enriched terms (Dataset S2). The number of exclusively enriched terms was larger than any shared terms (Fig. 4*B*). To identify which expression patterns, as identified in the *Control* group, were absent (lost) in one or more of the *Defeated* subgroups and which were absent in the *Control* group but identified (gained) in one or more of the subgroups, we overlapped all identified enriched terms for each subgroup with those of the *Control* group (note that the terms "loss" and "gain" reflect change of expression pattern and not of function). In all the three subgroups, there was more of gained than lost expression patterns (Fig. 4 *C*–*E*).

Discussion

Discovering cross-species resilience mechanisms requires translationally valid animal models. We designed an experimental approach that is aligned with findings from human research. Specifically, we propose threat–safety discrimination and responsiveness to extinction of aversive memories as resilience-associated signatures, while aversive response generalization and resistance to extinction as phenotypic characteristics of susceptibility. Second, we identified unique DEGs and gene networks in key brain regions of the fear circuitry underlying the established resilient and susceptible behavioral phenotypes.

To date, animal experimental research into resilience mechanisms has been largely built on a single phenotypic readout, namely CSD-induced social avoidance toward a mouse displaying the phenotypic characteristics of the aggressors' strain, as assessed during a social interaction test (20–22). The underlying hypothesis is that social avoidance after CSD reflects a generalized aversive response toward social contacts. The behavioral stratification developed here builds on our recent finding that at a group level, CSD-induced social avoidance is an aversive conditioned response that is specific to the phenotypic characteristics of the aggressors' strain serving as the threat-associated cue (18). The simultaneous presentation of two phenotypically distinct mouse strains in the STST, with one being from the aggressors' strain, allows the simultaneous assessment of CSD-induced social

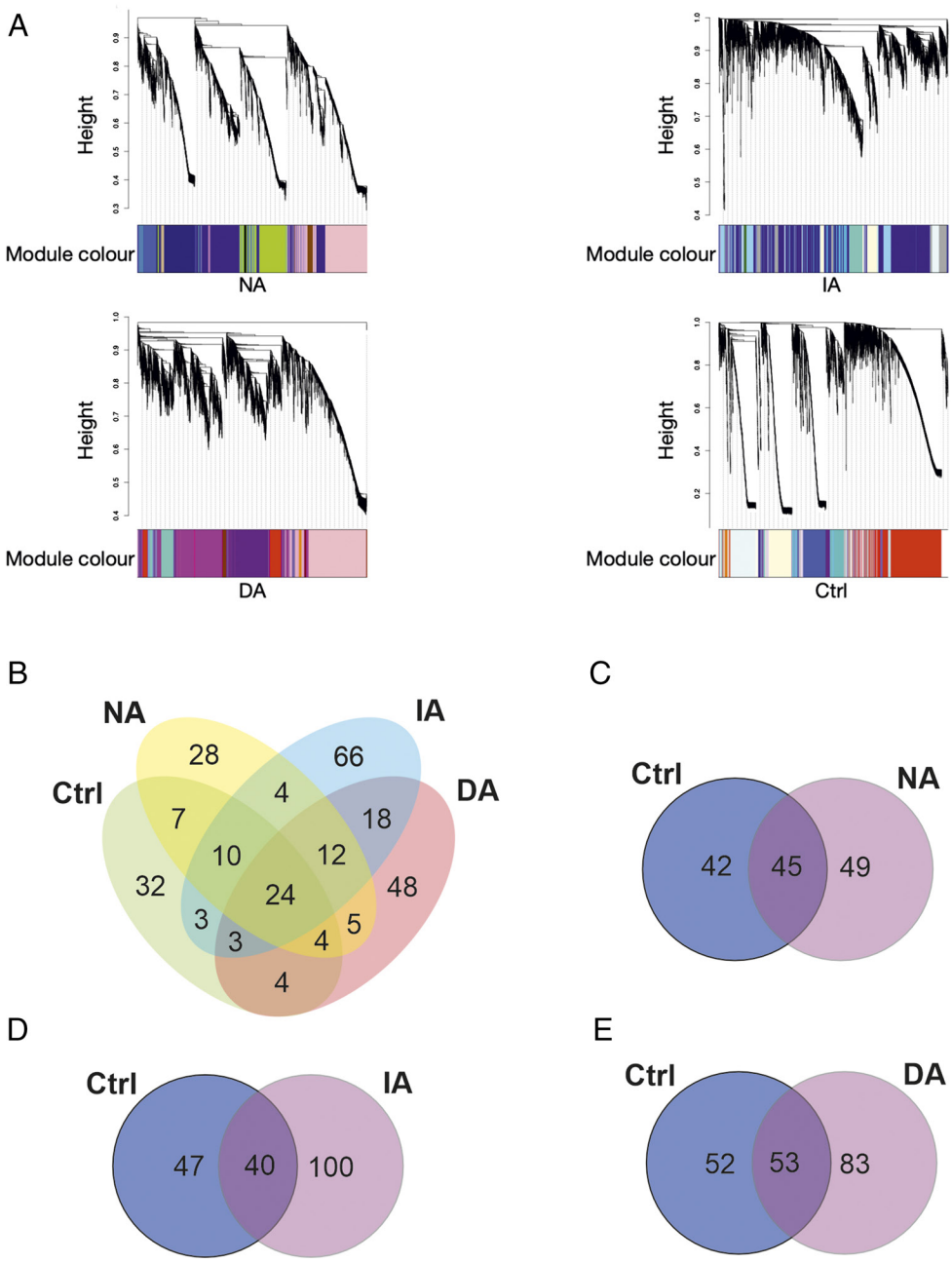

Fig. 4. Subgroup-specific gene coexpression networks. (*A*) *Defeated* subgroups exhibit a considerably different similarity structure of modules: Gene expression similarity structure across modules of coexpressed genes identified within the three different *Defeated* subgroups and the *Control* (Ctrl) group. Height of the dendrogram corresponds to dissimilarity of gene expression profiles across samples from all animals (lower value=more similar) used for clustering genes into modules. Colors of modules are arbitrarily assigned within each subgroup. (*B*) More subgroup-specific functionally enriched terms of modules than shared: While 24 terms are shared across all subgroups, 32 terms are specific to the *Control* (Ctrl) group and between 28 and 66 terms are specific to one of the three *Defeated* subgroups. (*C*–*E*) Unique numbers of functionally enriched terms of modules between the *Control* group and each of the three *Defeated* subgroups: *Control* (Ctrl) group-specific terms seen as "lost" in the respective *Defeated* subgroup, and *Defeated* subgroup-specific terms seen as "gained." Note that the terms "loss" and "gain" reflect change of expression pattern and not of function. *Non-avoiders* (NA) n = 17, *Indiscriminate-avoiders* (IA) n = 19, *Discriminating-avoiders* (DA) n = 15, and *Control* (Ctrl) n = 15.

avoidance toward the aggressors' strain *and* social threat–safety discrimination. Generating appropriate defensive behaviors when facing threat-associated stimuli is essential for survival, while withholding those behaviors when facing safe stimuli is adaptive. The characteristics of the *Discriminating-avoiders,* i.e., successful learning of threat-associated cues, threat–safety discrimination, and responsiveness to extinction of negative memories, are all discussed as characteristics of stress-resilient individuals (7). In contrast, generalized aversive responses and resistance to extinction after the occurrence of traumatic events, as seen by the *Indiscriminate-avoiders*, are key symptoms of stress-related mental disorders such as anxiety disorders (7, 23–35) and thus, are characteristic of stress-susceptible individuals (Fig. 2). Additionally, similar to the *Indiscriminate-avoiders*, generalized fear to nonthreatening situations in patients suffering from anxiety disorders (17) is not attributed to decreased fear response to the threat-associated cue, but a fear response to the safety signal itself (7, 23, 27–31).

Having established behavioral signatures driven by key brain regions of the fear circuitry, we aimed to gain insights into the underlying neurobiology by exploring transcriptional regulation in those regions. Therefore, we combined our behavioral phenotyping

with a brain region- and subgroup-specific differential expression analysis and identifying subgroup-specific coexpression networks.

In the mPFC, most DEGs specific to the stress-susceptible *Indiscriminate-avoiders* subgroup were hemoglobin-associated transcripts and genes encoding for proteins involved in vascular integrity and function. According to a recent meta-analysis, hemoglobin genes are among the most consistently regulated genes following a 10-d CSD (32). Hemoglobin expression is present in neurons (33), and recent findings suggest their specific involvement in neurodegenerative disorders (34). Additionally, chronic social stress may disrupt vascular integrity which in turn impairs blood flow and blood–brain barrier function (35, 36), among others (37, 38). Therefore, the vascular system may represent a mechanistic link underlying the comorbidity between stress, cardiovascular risk (39), and depression. Moreover, the *Indiscriminate-avoiders* subgroup showed, in the mPFC, exclusive regulation of complement C2 (*C2*). Members of the complement component family play a crucial role in neuroinflammation and behavior in mice under chronic stress conditions (40). In the vHC, the single specific DEG associated with the *Indiscriminate-avoiders* subgroup was hypocretin neuropeptide precursor (*Hcrt*). This gene encodes a neuropeptide precursor protein that gives rise to orexin A and orexin B. Literature points to the involvement of the orexinergic system in the development and progression of depressive-like phenotypes (41) and responses to stress (42). Previous work has shown that during 10 d of CSD, orexinergic neurons show increased activation (43). Thus, altered activation of orexinergic neurons may contribute to the development of chronic stress-induced maladaptive behaviors. Finally, the *Indiscriminate-avoiders* subgroup, which is characterized by, among others, resistance to extinction, displayed the most distinct transcriptional profile in the blA, a region involved in the acquisition, prevention, and attenuation of extinction (44, 45).

In the vHC, exclusively DEGs in the stress-resilient *Discriminating-avoiders* subgroup included, among others, gastric inhibitory polypeptide receptor (*Gipr*) and cholinergic receptor muscarinic 5 (*Chrm5*). The majority of publications focus on GIPR's role in metabolism (46), but there is evidence that anxiety-related behavior can be modulated via GIPR (47). Meanwhile, cholinergic signaling in the HC has been described to modulate social stress resilience in mice (48).

Next, we employed WGCNA. WGCNA is helpful in identifying transcriptional changes underlying complex mental disorder phenotypes where the phenotypic characteristics result from the convergence of multiple small changes rather than isolated effects of individual genes (49). Here, all *Defeated* subgroups exhibited a considerably different similarity structure of modules compared to the *Control* group and showed subgroup-specific patterns, supporting the concept that resilience is not simply the absence of susceptibility, but a distinct and dynamic process.

Overall, the transcriptomic findings suggest that the subgroups display distinct signatures of DEGs and gene coexpression networks in key brain regions of the fear circuitry underlying their respective behavioral signature. Our transcriptome analysis should be interpreted as exploratory. A limitation may arise from differential expression analysis using simple two-group comparison. Statistical models applied to the full dataset treating CSD and the behavioral stratification as two independent factors may reveal additional expression patterns. Future analyses separating the mPFC and the vHC into subregions or targeting specific neuronal populations may provide refined insights into the transcriptional signatures underlying the behavioral model. Furthermore, future studies integrating subgroup-specific transcriptional signatures reported here with systematically obtained brain structural information on the three *Defeated* subgroups will greatly contribute to a better understanding of the model.

Taken together, we establish a translationally informed and fear circuit-based framework in mice following chronic social stress for the identification of resilient phenotypes based on the ability of threat–safety discrimination and responsiveness to the extinction of aversive memories, both of which are important in fine-tuning individual responses to stress and mental health outcomes (5). The combination of fear circuit-based neurobehavioral analyses with transcriptomics has allowed us to substantiate the biological relevance of the proposed phenotypic stratification and explore potential target genes for promoting a resilient phenotype. Our approach substantially refines the currently used dichotomous behavioral classification into resilient and susceptible individuals and holds great potential for future studies to decode the neurobiological mechanisms of resilience. Our results may also instruct the refinement of prevention strategies, for example, stress inoculation training (50, 51), and inform the development of individualized treatment strategies to stress-related mental disorders.

Materials and Methods

Animals. C57BL/6J male mice (n = 207) weighing 22 to 28 g at the age of seven weeks were obtained from Janvier (France) and housed individually in a temperature- and humidity- controlled facility on a 12 h light–dark cycle (23 °C, 38%, lights on 8:00) with ad libitum. Procedures were performed in accordance with the European Communities Council Directive and approved by local authorities (Landesuntersuchungsamt Rheinland-Pfalz).

CSD. The treatment was performed as previously described (52). For 10 d, experimental mice (*Defeated* n = 165) were introduced into the home cage of a larger, older, and retired male breeder from the aggressor's strain (CD-1). After physical defeat, animals were separated by a mesh wall overnight. During the same period, age-matched mice randomized to the nondefeated group (*Control* n = 42) were handled (*SI Appendix*). On the last day, all mice were housed individually in new cages to rest overnight. The following tests were conducted between 8:30 and 13:30 under light conditions of 37 lx.

STST. The test was performed similar to Ayash and colleagues (18). In brief, the experimental mice were introduced in a three-chambered arena, where each of the two peripheral chambers contained an empty mesh enclosure. After 6 min of habituation phase, a 6-min testing phase immediately followed with two larger, older, and novel mice from different strains (CD-1 aggressors' strain and 129/Sv novel strain) simultaneously presented in each enclosure (Fig. 1*A*). Using the *social interaction index* (Fig. 1*B*), we identified three phenotypic subgroups within the *Defeated* group. For tracking details, see *SI Appendix*.

Active Avoidance Task. The test was performed for seven consecutive days with 20 cycles/animal/day in active avoidance boxes by TSE Systems GmbH, Bad Nauheim, Germany. Activity was detected by infrared beams. The animals underwent 60 s of habitation followed by 10 kHz tone. Then, only for animals that did not change sides within 5 s, a foot shock of 0.4 mA was administered until sides were changed (if no change, until 10 s), 30 s intertrial interval (ITI) followed. Time to change sides is a measurement of conditioned avoidance response.

Social Avoidance Extinction Training. The training was performed similar to Ayash and colleagues (18). In brief, animals alternated between the same cages of the previously encountered CD-1 aggressors during the CSD for 15 min/d for 16 consecutive days with a mesh wall in-between (only sensory contact) before returning to their home cages (Fig. 1*F*).

Transcriptome Analysis. To explore transcriptional signatures that underlie the respective subgroup-specific behavioral characteristics, selected animals had social interaction indices around the mean value of the respective subgroup with each of the two strains. Animals were killed by isoflurane inhalation followed by decapitation, brains were extracted instantaneously, frozen in methylbutane, and stored at −80 °C. For tissue punching, RNA isolation, NGS library preparation, and transcriptome analysis, see *SI Appendix*.

The transcriptome data have been deposited in NCBI's Gene Expression Omnibus (GSE161726, ref. 53).

Behavioral Statistical Analysis. Analyses were performed using GraphPad Prism 8, two sided, and parametric. Appropriate statistical tests were chosen followed by outlier analysis Grubb's test $P \leq 0.05$. Similar variance was confirmed before analysis. Time was calculated in percent of total time of the respective test (time%). See figure legends for details.

Data, Materials, and Software Availability. Raw RNA sequencing reads and gene counts data have been deposited in NCBI gene expression omnibus (GEO) (GSE161726) (54). All study data are included in the article and/or supporting information.

ACKNOWLEDGMENTS. This work was supported by the Deutsche Forschungsgemeinschaft (CRC 1193, B01, C01, Z02) and the Boehringer Ingelheim Foundation (individual phenotyping and high-resolution automated behavioral analysis). We thank Dr. Radyushkin, Dr. Sillaber, Ms. Reichel, Mr. Schmitz, Dr. Carboncino, Ms. Deuster, Ms. Klüpfel, and Ms. Opitz for their technical assistance. We thank Dr. Mendez-Lago and Ms. Lukas (Genomics Core Facility, Institute of Molecular Biology, Mainz, Germany) for their support with next-generation sequencing. We would also like to thank Prof. Christian Lüscher (University of Geneva) for contributing his time and knowledge into the work. *Chronic Social Defeat*, *Social Threat-Safety Test*, and *Social Avoidance Extinction Training* depictions were adapted from icons by BioRender.com. The funding sources had no involvement in the study.

Author affiliations: [a]Leibniz Institute for Resilience Research, Mainz 55122, Germany; [b]Translational Psychiatry, Department of Psychiatry and Psychotherapy, University Medical Center Mainz, Mainz 55128, Germany; [c]Genevention GmbH, Göttingen 37079, Germany; [d]Department of Basic Neuroscience, University of Geneva, Geneva 1205, Switzerland; [e]Institute for Human Genetics, University Medical Center Mainz, Johannes Gutenberg University Mainz, Mainz 55128, Germany; [f]Living Systems Institute and Department of Clinical and Biomedical Sciences, University of Exeter, Exeter EX4 4QD, United Kingdom; and [g]Neuroimaging Center, Focus Program Translational Neuroscience, Johannes Gutenberg University Medical Center Mainz, Mainz 55131, Germany

Author contributions: S.A. conceived the idea; S.A., U.S. and M.B.M. developed the conceptual framework and interpreted the results; S.A. planned and carried out the experiments, performed the behavioural analysis, T.L. and A.R. performed the bioinformatic analyses, S.A. and S.R. supported the bioinformatic analysis, R.K., U.S., and M.B.M. verified the analytical methods, R.K. supported the results interpretation. All authors contributed to the writing and revising of the manuscript.

1. Global Burden of Disease Study 2013 Collaborators, Global, regional, and national incidence, prevalence, and years lived with disability for 301 acute and chronic diseases and injuries in 188 countries, 1990–2013: A systematic analysis for the Global Burden of Disease Study 2013. *Lancet* **386**, 743–800 (2015).
2. G. A. Bonanno, M. Westphal, A. D. Mancini, Resilience to loss and potential trauma. *Annu. Rev. Clin. Psychol.* **7**, 511–535 (2011).
3. R. Kalisch *et al.*, The resilience framework as a strategy to combat stress-related disorders. *Nat. Hum. Behav.* **1**, 784–790 (2017).
4. L. J. Chang, M. Reddan, Y. K. Ashar, H. Eisenbarth, T. D. Wager, The challenges of forecasting resilience. *Behav. Brain Sci.* **38**, e98 (2015).
5. I. M. Veer *et al.*, Psycho-social factors associated with mental resilience in the Corona lockdown. *Transl. Psychiatry* **11**, 1–11 (2021).
6. R. Kalisch, M. B. Müller, O. Tüscher, A conceptual framework for the neurobiological study of resilience. *Behav. Brain Sci.* **38**, e92 (2015).
7. P. Duits *et al.*, Updated meta-analysis of classical fear conditioning in the anxiety disorders. *Depression Anxiety* **32**, 239–253 (2015).
8. M. Brunetti *et al.*, Elevated response of human amygdala to neutral stimuli in mild post traumatic stress disorder: Neural correlates of generalized emotional response. *Neuroscience* **168**, 670–679 (2010).
9. S. J. Diener *et al.*, Reduced amygdala responsivity during conditioning to trauma-related stimuli in posttraumatic stress disorder. *Psychophysiology* **53**, 1460–1471 (2016).
10. T. Jovanovic *et al.*, Posttraumatic stress disorder may be associated with impaired fear inhibition: Relation to symptom severity. *Psychiatry Res.* **167**, 151–160 (2009).
11. T. Jovanovic *et al.*, Fear potentiation and fear inhibition in a human fear-potentiated startle paradigm. *Biol. Psychiatry* **57**, 1559–1564 (2005).
12. S. Lissek *et al.*, Overgeneralization of conditioned fear as a pathogenic marker of panic disorder. *Am. J. Psychiatry* **167**, 47–55 (2010).
13. S. D. Norrholm *et al.*, Conditioned fear extinction and reinstatement in a human fear-potentiated startle paradigm. *Learn. Mem.* **13**, 681–685 (2006).
14. M. S. Sep, A. Steenmeijer, M. Kennis, The relation between anxious personality traits and fear generalization in healthy subjects: A systematic review and meta-analysis. *Neurosci. Biobehav. Rev.* **107**, 320–328 (2019).
15. A. N. Kaczkurkin *et al.*, Neural substrates of overgeneralized conditioned fear in PTSD. *Am. J. Psychiatry* **174**, 125–134 (2017).
16. S. P. Cahill, E. B. Foa, "Psychological theories of PTSD" in *Handbook of PTSD: Science and Practice*, M. J. Friedman, T. M. Keane, P. A. Resick, Eds. (The Guilford Press, 2007), pp. 55–77.
17. J. N. Krueger, S. Sangha, On the basis of sex: Differences in safety discrimination vs. conditioned inhibition. *Behav. Brain Res.* **400**, 113024 (2021).
18. S. Ayash, U. Schmitt, M. B. Müller, Chronic social defeat-induced social avoidance as a proxy of stress resilience in mice involves conditioned learning. *J. Psychiatr. Res.* **120**, 64–71 (2020).
19. D. Murra *et al.*, Characterizing the behavioral and neuroendocrine features of susceptibility and resilience to social stress. *Neurobiol. Stress* **17**, 100437 (2022).
20. S. A. Golden, H. E. Covington, O. Berton, S. J. Russo, A standardized pro- tocol for repeated social defeat stress in mice. *Nat. Protoc.* **6**, 1183–1191 (2011).
21. O. Berton *et al.*, Essential role of BDNF in the mesolimbic dopamine pathway in social defeat stress. *Science* **311**, 864–868 (2006).
22. V. Krishnan *et al.*, Molecular adaptations underlying susceptibility and resistance to social defeat in brain reward regions. *Cell* **131**, 391–404 (2007).
23. C. Grillon, C. A. Morgan, Fear-potentiated startle conditioning to explicit and contextual cues in Gulf War veterans with posttraumatic stress disorder. *J. Abnormal Psychol.* **108**, 134–142 (1999).
24. C. R. Brewin, A cognitive neuroscience account of posttraumatic stress disorder and its treatment. *Behav. Res. Therapy* **39**, 373–393 (2001).
25. M. R. Milad, S. L. Rauch, R. K. Pitman, G. J. Quirk, Fear extinction in rats: Implications for human brain imaging and anxiety disorders. *Biol. Psychol.* **73**, 61–71 (2006).
26. T. Jovanovic, S. D. Norrholm, Neural mechanisms of impaired fear inhibition in posttraumatic stress disorder. *Front. Behav. Neurosci.* **5**, 44 (2011).
27. G. A. Bonanno, Loss, trauma, and human resilience: Have we underestimated the human capacity to thrive after extremely aversive events? *Am. Psychol.* **59**, 20–28 (2004).
28. K. G. Coifman, G. A. Bonanno, E. Rafaeli, Affect dynamics, bereavement and resilience to loss. *J. Happiness Stud.* **8**, 371–392 (2007).
29. C. E. Waugh, R. J. Thompson, I. H. Gotlib, Flexible emotional responsiveness in trait resilience. *Emotion* **11**, 1059–1067 (2011).
30. G. A. Bonanno, Resilience in the face of potential trauma. *Curr. Directions Psychol. Sci.* **14**, 135–138 (2005).
31. R. Yehuda, J. D. Flory, S. Southwick, D. S. Charney, Developing an agenda for translational studies of resilience and vulnerability following trauma exposure. *Ann. NY Acad. Sci.* **1071**, 379–396 (2006).
32. V. V. Reshetnikov, P. E. Kisaretova, N. P. Bondar, Transcriptome alterations caused by social defeat stress of various durations in mice and its relevance to depression and posttraumatic stress disorder in humans: A meta-analysis. *Int. J. Mol. Sci.* **23**, 13792 (2022).
33. M. Biagioli *et al.*, Unexpected expression of α-and β-globin in mesencephalic dopaminergic neurons and glial cells. *Proc. Natl. Acad. Sci. U.S.A.* **106**, 15454–15459 (2009).
34. B. A. Killinger *et al.*, In situ proximity labeling identifies Lewy pathology molecular interactions in the human brain. *Proc. Natl. Acad. Sci. U.S.A.* **119**, e2114405119 (2022).
35. C. Menard *et al.*, Social stress induces neurovascular pathology promoting depression. *Nat. Neurosci.* **20**, 1752–1760 (2017).
36. K. A. Dudek *et al.*, Molecular adaptations of the blood–brain barrier promote stress resilience vs. depression. *Proc. Natl. Acad. Sci. U.S.A.* **117**, 3326–3336 (2020).
37. D. I. Bink, K. Ritz, E. Aronica, L. Van Der Weerd, M. J. Daemen, Mouse models to study the effect of cardiovascular risk factors on brain structure and cognition. *J. Cerebral Blood Flow Metab.* **33**, 1666–1684 (2013).
38. P. W. Pires, C. M. Dams Ramos, N. Matin, A. M. Dorrance, The effects of hypertension on the cerebral circulation. *Am. J. Physiol. Heart Circ. Physiol.* **304**, H1598–H1614 (2013).
39. M. Kivimäki, A. Steptoe, Effects of stress on the development and progression of cardiovascular disease. *Nat. Rev. Cardiol.* **15**, 215–229 (2018).
40. S. Tripathi *et al.*, Type 1 interferon mediates chronic stress-induced neuroinflammation and behavioral deficits via complement component 3-dependent pathway. *Mol. Psychiatry* **26**, 3043–3059 (2021).
41. M. H. James, E. J. Campbell, C. V. Dayas, Role of the Orexin/Hypocretin System in Stress-Related Psychiatric Disorders. *Curr Top Behav Neurosci.* **33**, 197–219 (2017).
42. L. A. Grafe, S. Bhatnagar, Orexins and stress. *Front. Neuroendocrinol.* **51**, 132–145 (2018).
43. D. Wang *et al.*, Lateral hypothalamus orexinergic inputs to lateral habenula modulate maladaptation after social defeat stress. *Neurobiol. Stress* **14**, 100298 (2021).
44. C. L. Wellman, K. M. Moench, Preclinical studies of stress, extinction, and prefrontal cortex: Intriguing leads and pressing questions. *Psychopharmacology* **236**, 59–72 (2019).
45. I. Akirav, H. Raizel, M. Maroun, Enhancement of conditioned fear extinction by infusion of the GABAA agonist muscimol into the rat prefrontal cortex and amygdala. *Eur. J. Neurosci.* **23**, 758–764 (2006).
46. R. J. Samms, K. W. Sloop, F. M. Gribble, F. Reimann, A. E. Adriaenssens, GIPR function in the central nervous system: Implications and novel perspectives for GIP-based therapies in treating metabolic disorders. *Diabetes* **70**, 1938–1944 (2021).
47. X.-S. Wang *et al.*, Activation of GIPR exerts analgesic and anxiolytic-like effects in the anterior cingulate cortex of mice. *Front. Endocrinol.* **13**, 887238 (2022).
48. Y. S. Mineur *et al.*, Cholinergic signaling in the hippocampus regulates social stress resilience and anxiety-and depression-like behavior. *Proc. Natl. Acad. Sci. U.S.A.* **110**, 3573–3578 (2013).
49. C. Gaiteri, Y. Ding, B. French, G. C. Tseng, E. Sibille, Beyond modules and hubs: The potential of gene coexpression networks for investigating molecular mechanisms of complex brain disorders. *Genes. Brain Behavior.* **13**, 13–24 (2014).
50. S. Ayash, U. Schmitt, D. M. Lyons, M. B. Müller, Stress inoculation in mice induces global resilience. *Translat. Psychiatry* **10**, 1–8 (2020).
51. R. Yuan *et al.*, Long-term effects of intermittent early life stress on primate prefrontal–subcortical functional connectivity. *Neuropsychopharmacology* **46**, 1348–1356 (2021).
52. M. A. van der Kooij *et al.*, Chronic social stress-induced hyperglycemia in mice couples individual stress susceptibility to impaired spatial memory. *Proc. Natl. Acad. Sci. U.S.A.* **115**, E10187–E10196 (2018).
53. R. Edgar, M. Domrachev, A. E. Lash, Gene Expression Omnibus: NCBI gene expression and hybridization array data repository. *Nucleic Acids Res.* **30**, 207–210 (2002).
54. S. Ayash *et al.*, Reconceptualising resilience within a translational framework is supported by unique and brain-region specific transcriptional signatures in mice. Gene Expression Omnibus. https://www.ncbi.nlm.nih.gov/geo/query/acc.cgi?acc=GSE161726. Deposited 18 November 2020.